Imaging Alzheimer's disease-related protein aggregates in human cells using a selenium label

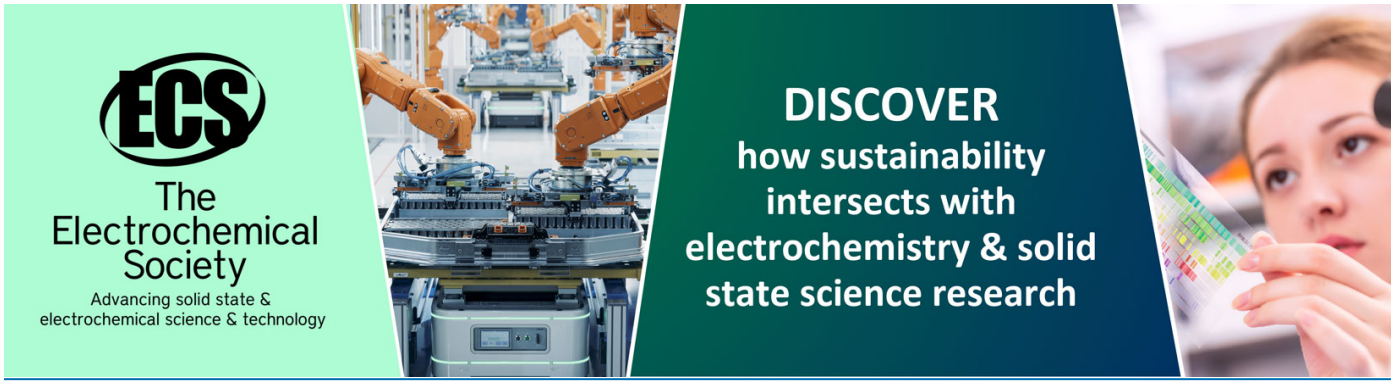

Journal of Physics: Conference Series **241** (2010) 012020 doi:10.1088/1742-6596/241/1/012020

Imaging Alzheimer's disease-related protein aggregates in human cells using a selenium label

E K McGuire[1], M Motskin[2], T P J Knowles[3], C M Dobson[4], D W McComb[1] and A E Porter[1]

[1] Dept. of Materials, Imperial College, Exhibition Rd, London SW7 2AZ, UK
[2] Dept. of Anatomy, University of Cambridge, Downing St, Cambridge CB2 3DY, UK
[3] Nanoscience Centre, University of Cambridge, JJ Thomson Ave, Cambridge, CB3 0FF, UK
[4] Dept. of Chemistry, University of Cambridge, Lensfield Rd, Cambridge CB2 1EW, UK

Email: e.mcguire07@imperial.ac.uk

Abstract. The aberrant folding and subsequent aggregation of proteins and peptides is associated with a range of pathological conditions from the systemic amyloidoses to neurodegenerative diseases such as Alzheimer's and Parkinson's diseases. While this link is well established there is a lack of understanding of the exact role protein aggregates play in disease pathogenesis. Part of the reason for this is that it has proved extremely challenging to characterise the localisation and structure of amyloid fibrils within the cellular environment due to a lack of contrast between the carbon rich protein aggregates and the carbon rich cell. We report a novel method for visualising Alzheimer's disease-related amyloid fibrils inside human cells without the use of invasive or unreliable stains or tags. The naturally occurring sulfur atom in the amyloid-β peptide is replaced with a selenium atom, a heavier element in the same group of the periodic table of elements. Using high angle annular dark field (HAADF) in a scanning transmission electron microscopy (STEM) the selenium-labelled aggregates can be identified within the cellular environment.

The aberrant folding and subsequent aggregation of proteins and peptides into insoluble plaques known as amyloid fibrils[1, 2] is associated with a number of diseases including the systemic amyloidoses, Alzheimer's and Parkinson's diseases and late onset diabetes[1, 3, 4]. Although recent research has revealed increasingly detailed molecular events associated with the formation of such aggregates[5, 6], the localisation of these structures within the cell and the detailed mechanisms that characterise their involvement in disease states are crucial questions which largely remain to be addressed[7]. The challenges in providing answers to such questions originate from difficulties in imaging carbon containing polypeptide aggregates within the carbon rich cell[8]. Previous strategies for overcoming this lack of contrast have involved the use of potentially intrusive tags or of heavy element stains that have an extremely low level of specificity.

In this paper an alternative approach for increasing selectively the contrast of intracellular peptide aggregates by labelling the fibrils in such a way as to increase their scattering power relative to the cellular environment is described. The selenium analogue of the sulfur-containing amino acid

methionine, which possesses a larger electron scattering cross section than its natural counterpart but is chemically essentially identical to it has been incorporated into the peptide. The samples were imaged using high angle annular dark field (HAADF) imaging in the scanning transmission electron microscope (STEM). This technique is highly sensitive to local variations in the atomic number within the sample because of the Z^n-dependency of Rutherford scattering [9].

The aggregation and toxicity of a peptide corresponding to residues 25-36 human amyloid-β (Aβ) protein, the main constituent of the plaques found in the brains of Alzheimer's patients[2], and from an analogous peptide in which the methionine residue in position 35 is replaced by its selenium-labelled analogue. The protein was prepared by dissolution in trifluoroacetic acid followed by lyophilisation and dissolution in 1,1,1,3,3,3-hexafluoro-2-propanol. The protein was then diluted in phosphate buffered saline at pH7.4 with 100mM NaCl at a protein concentration of 100μM at 37°C. The aggregation was examined using thioflavin-T fluorescence and transmission electron microscopy (TEM); branched, globular aggregates were formed after three hours and longs thin amyloid fibrils were formed after about 12 hours. Human monocyte derived macrophage cells (HMMs) were exposed to the aggregates at a concentration of 10μM for varying lengths of time from 2 to 24 hours before fixation, according to a protocol published previously[10]. Samples were then ultramicrotomed into thin sections (40 – 250nm) and mounted on 300 mesh bare copper grids for examination by HAADF-STEM. No formvar or carbon support films were used in order to minimise the total sample thickness. HAADF-STEM experiments were performed on an FEI Titan microscope operating at 300kV with a convergence angle of 14mrad and a probe size of approximately 0.24nm.

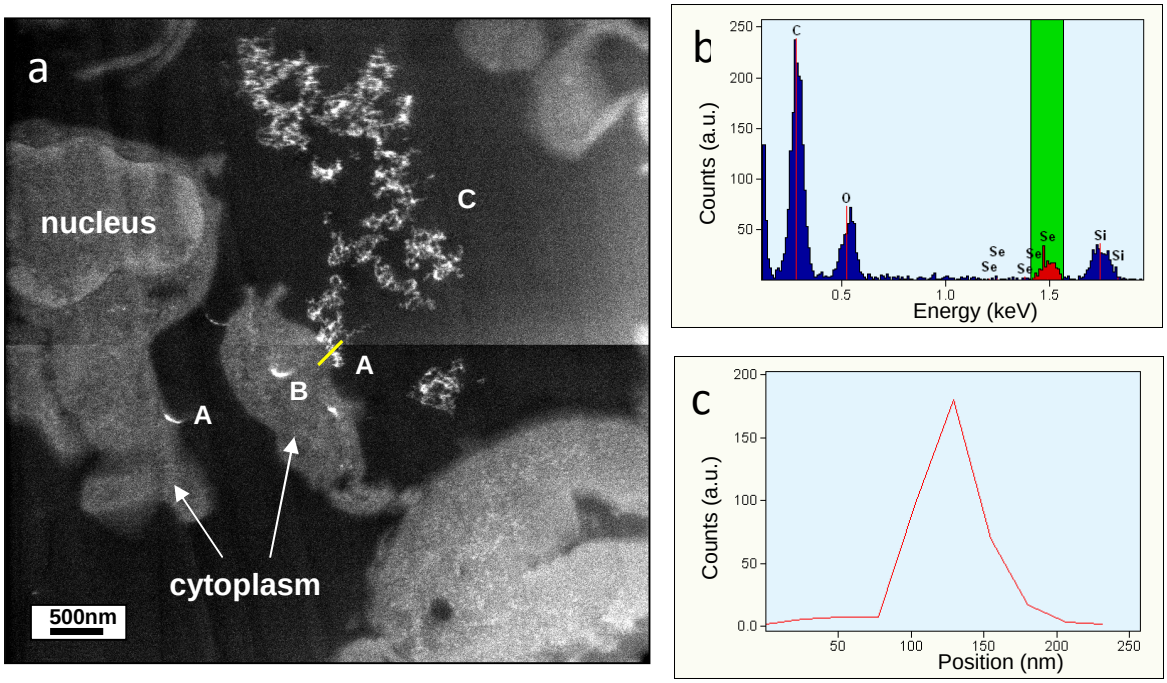

Figure 1: (a) HAADF-STEM image of HMMs exposed to selenium-labelled fibrils showing fibrils associated with the cell membrane, A, in the cell cytoplasm, B, and in the extracellular space, C. The line indicates the fibril across which an EDX line spectrum image (SI) was recorded. (b) The EDX spectrum at the point of highest concentration of selenium and highest HAADF signal on the line SI. (c) Selenium profile extracted from SI.

Figure 1a shows a HAADF-STEM image recorded with inner (θ_{in}) and outer (θ_{out}) HAADF collection angles of 12.8mrad and 63.7mrad respectively, showing selenium-labelled fibrils associated

with the cell membrane, A, in the cell cytoplasm, B, and in the extracellular space, C. To confirm that the observed increased scattering is due to the selenium atoms incorporated into the fibrils an energy dispersive X-ray (EDX) spectrum image was recorded across the fibril image (figure 1c). Figure 1b shows the EDX spectrum at the HAADF peak and clearly shows the presence of selenium. The total counts for an energy window around the selenium peak across the spectrum image is shown in figure 1c and shows that the highest concentration of selenium corresponds with the highest intensity of electrons falling on the HAADF detector showing that the increased intensity at the position of the fibrils is indeed due to the presence of selenium.

For biological samples mass-thickness is the "conventional" source of contrast when imaging in the electron microscope. If θ_{in} is small then the HAADF image will be dominated by mass-thickness contrast (figure 2a). As θ_{in} is increased the contribution to the HAADF image from electrons that have undergone Rutherford scattering is increased while the contribution from mass-thickness contrast is reduced. At high θ_{in} the HAADF image is dominated by electrons that have undergone Rutherford scattering (figure 2b); this means that the main source of contrast in the image is due to local variations in atomic number. The low collection angles used when recording figure 2a allow cell organelles such as the nucleus to be identified, due to variations in sample density, as well as the selenium-labelled fibrils. The higher collection angles used when recording figure 2b mean that cell organelles are not visible whereas the selenium-labelled fibrils can be identified. This method allows the fibrils to be identified within the cellular environment without the use of any other staining thanks to the incorporated selenium atom.

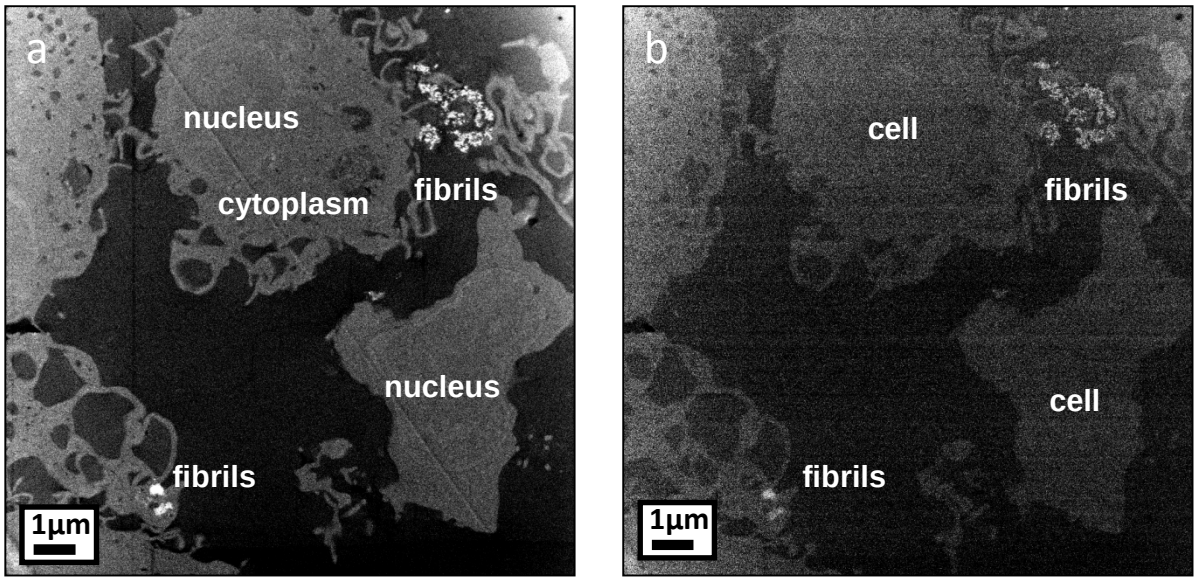

Figure 2: (a) HAADF-STEM image of HMMs exposed to selenium-labelled fibrils recorded with θ_{in} 8.3mrad and θ_{out} 41.5mrad. (b) HAADF-STEM image of the same area of the sample recorded with θ_{in} 32.5mrad and θ_{out} 161.0mrad. Both images were recorded using a probe size of approximately 0.24nm.

3-D electron tomography was performed on selected sections of cells exposed to the Se-peptide in order to visualise the distribution of protein aggregates in three dimensions. HAADF-STEM tomographic datasets were acquired over a tilt range of -36° to +42° using a step size of 2°. For these STEM-tomography measurements, we used samples of 250 nm thickness in order to increase volume information. Three-dimensional reconstruction was carried out using the simultaneous iterative reconstruction technique[11, 12] using EMISPEC 3-D reconstruction software; reconstructed images were visualised in slices using AmiraTM 3D visualization software. Figure 3a shows a HAADF-STEM image of a selenium-labelled aggregate which has entered the cell cytoplasm from the

extracellular medium. Figure 3b shows a Voltex 3D reconstruction of the boxed area in figure 3a showing that the aggregates are inside the cell cytoplasm.

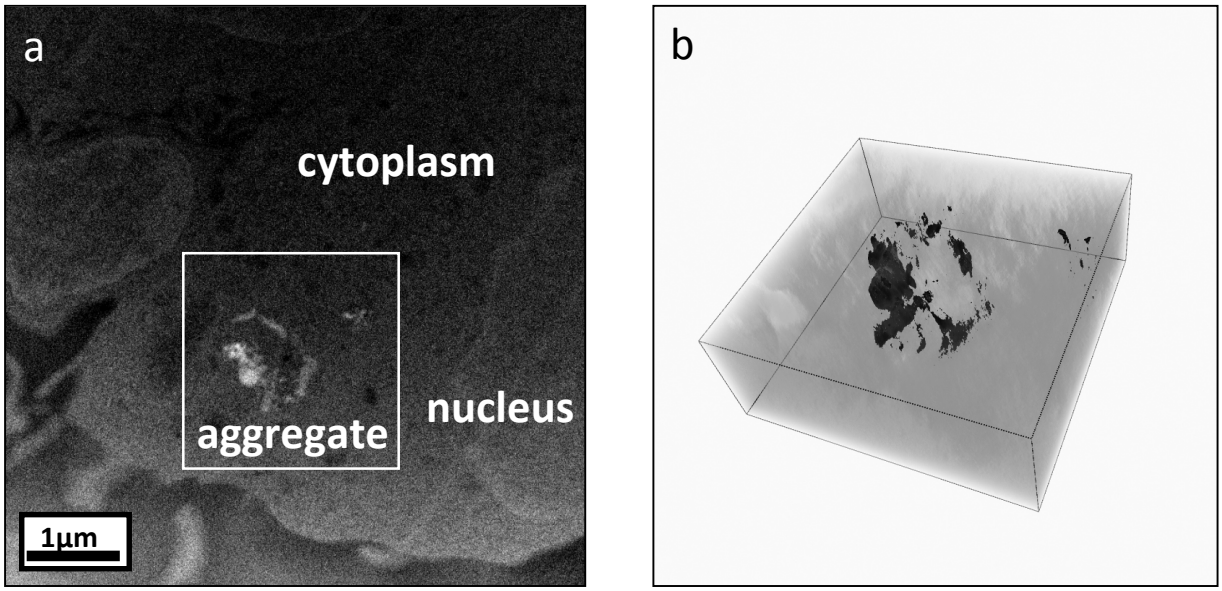

Figure 3: (a) HAADF-STEM image of a selenium-labelled aggregate in the cell cytoplasm. (b) Voltex 3D reconstruction of a HAADF-STEM tomography series taken of the boxed region in (a).

In conclusion, the results of this study show that the use of peptides in which the natural sulfur atoms are replaced with selenium enables the observation of amyloid fibrils within individual cells and cell compartments. This approach therefore represents a powerful tool for future investigations of the molecular processes that underlie the normal and aberrant effects of protein self-assembly and misassembly in living systems.

References

1. Chiti, F. and C.M. Dobson, Annual Review of Biochemistry, 2006. **75**: p. 333-366.
2. Dobson, C.M., Nature, 2003. **426**(6968): p. 884-890.
3. Pepys, M.B. *Pathogenesis, diagnosis and treatment of systemic amyloidosis*. in *Discussion Meeting on Protein Misfolding and Disease*. 2000. London, England.
4. Kelly, J.W., Nature Structural Biology, 2002. **9**(5): p. 323-325.
5. Wasmer, C., et al., Science, 2008. **319**(5869): p. 1523-1526.
6. Collins, S.R., et al., Plos Biology, 2004. **2**(10): p. 1582-1590.
7. Lansbury, P.T. and H.A. Lashuel, Nature, 2006. **443**(7113): p. 774-779.
8. Jensen, G.J., Science, 2009. **323**(5913): p. 472-473.
9. Eckman, C.B., et al., Human Molecular Genetics, 1997. **6**(12): p. 2087-2089.
10. Porter, A.E., et al., Acta Biomaterialia, 2006. **2**(4): p. 409-419.
11. Kak, A.C. and M. Slaney, *Principles of Computerized Tomographic Imaging*. 1988: IEEE Press.
12. Gilbert, P., J Theor Biol, 1972. **36**(1): p. 105-17.